Available online at www.sciencedirect.com
SCIENCE DIRECT®
C. R. Mecanique 333 (2005) 507–512
COMPTES RENDUS MECANIQUE
http://france.elsevier.com/direct/CRAS2B/

Crystallization, pore relaxation and micro-cryosuction in cohesive porous materials

Olivier Coussy, Teddy Fen-Chong

Institut Navier, LMSGC, 2, allée Kepler, 77420 Champs-sur-Marne, France

Received 16 September 2004; accepted 27 January 2005

Available online 5 May 2005

Presented by Évariste Sanchez-Palencia

Abstract

A poro-elastic analysis is undertaken to account for the pressure time history of water-infiltrated pores within a material subjected to freezing. The thermodynamic-mechanical equilibrium of undercooled water and ice crystal, and Poiseuille-like flow through the connection channels, combine to reveal three successive mechanisms: in-pore crystallization, in-pore partial melting and a micro-cryosuction process, driving liquid water from the yet unfrozen pores to the frozen sites. The model turns out to be apt to predict the macroscopic relaxation process observed at the onset of crystallization as reported in the literature for cement-based materials. ***To cite this article: O. Coussy, T. Fen-Chong, C. R. Mecanique 333 (2005).***

Résumé

Cristallisation, relaxation de pore, et cryosuccion. Une analyse poroelastisque est entreprise afin de rendre compte de l'évolution de la pression de pore dans un matériau soumis au gel. La prise en compte conjointe de l'équilibre à la fois thermodynamique et mécanique de l'eau surfondue et du cristal de glace, et d'un écoulement visqueux dans les canaux de connection, aboutit à la mise en évidence de trois mécanismes successifs : gel du pore, fonte partielle et cryosuccion, pompant l'eau des pores encore liquides vers les sites gelés. Le modèle s'avère capable de prédire le processus de relaxation macroscopique observé au début de la cristallisation tel que reporté dans la littérature pour les matériaux à base cimentaire. ***Pour citer cet article : O. Coussy, T. Fen-Chong, C. R. Mecanique 333 (2005).***

Keywords: Porous media; Pore pressure; Freezing; Crystallization; Melting; Relaxation; Undercooling; Cryosuction; Cement

Mots-clés : Milieux poreux ; Pression de pore ; Gel ; Cristallisation ; Fonte ; Relaxation ; Surfusion ; Cryosuccion ; Ciment

E-mail addresses: Olivier.Coussy@mail.enpc.fr (O. Coussy), teddy.fen-chong@lcpc.fr (T. Fen-Chong).

1631-0721/$ – see front matter
doi:10.1016/j.crme.2005.01.005

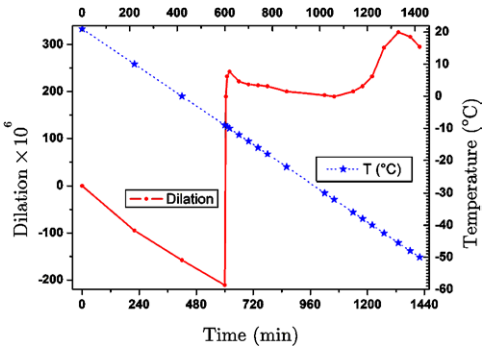

Fig. 1. Dilation of M50 cement paste samples (extracted from [8]). Cooling rate is 3 K/h. The sample expands for 20 min for a temperature decrease from 264 K to 263 K, then contracts (relaxes) for a temperature fall to 241 K. It expands again for temperature decrease down to 227 K before starting a new contraction stage.

1. Introduction

Upon freezing the mechanical behaviour of water-infiltrated materials is not governed by solely the mass density decrease accompanying water solidification, nor the temperature gradients. Indeed it has been experimentally observed by Beaudoin and MacInnis [1] that sealed cement paste samples, subjected to uniform increasing coolings, still expand if water is replaced by benzene which contracts when solidifying. Actually, at uniform temperatures well below the bulk freezing point ($T_f \simeq 273$ K at atmospheric zero pressure), confined water can remain liquid owing to intermolecular and surface forces (see for instance [2–4]). The resulting undercooling, by driving the yet unfrozen liquid water to the already frozen sites, builds up a pore pressure that can damage the material. As a result the durability of cement-based materials upon the action of frost has motivated extensive research work from pioneering work of Powers [5] to more recent studies [6,7]. By means of an intentionally simple think-model, this Note mainly aims at explaining this unexpected dilation, as well as the relaxation process which is macroscopically observed at the onset of crystallization in cement-based materials, see Fig. 1 from data reported in Fig. 3 of [8]. In these experiments, it must be pointed out that the sample dimensions are sufficiently small so that the characteristic time of thermal diffusion is much smaller than the characteristic time of cooling. As a consequence, in contrast to frost heave, the observed deformation occurs at a uniform temperature within the sample. Actually, it has long been recognized [9] that frost heave is due to temperature gradients operating at the larger scale of uncohesive soils layers.

2. Pore model

We consider the idealized pore model sketched in Fig. 2. A spherical pore of radius R is embedded within a linear elastic infinite medium. It is connected to the neighbouring porous network through thin cylindrical channels with radius $a \ll R$. It is also possibly connected to the material surface through a cylindrical pore with radius κ such as $a < \kappa < R$.

The porous element initially liquid water-saturated is subjected to a uniform temperature decreasing from T_f. The temperature T^* at which an ice crystal at pressure p_C with mean curvature radius r^* is in equilibrium with the neighbouring liquid water at pressure p_L, both mechanically (Young–Laplace law) and thermodynamically (equality of chemical potentials) is given by the Gibbs–Thomson equation

$$T^* = T_f - \frac{2\gamma}{r^* \mathcal{S}_f} \tag{1}$$

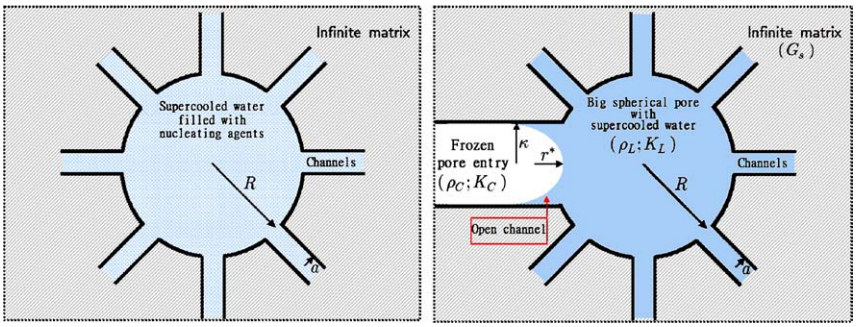

Fig. 2. Two possible freezing processes in a volume element of porous material: (a) in-pore homogeneous nucleation; (b) ice invasion.

where γ is the liquid/crystal interface energy and $\mathcal{S}_f$ the entropy of fusion per unit of crystal volume. The related undercooling $\Delta\mu^*$, that is, the difference between the potentials of undercooled water and ice at atmospheric pressure, satisfies

$$p_C - p_L = \mathcal{S}_f(T_f - T^*) = \rho_C^0 \Delta\mu^* > 0 \tag{2}$$

where ρ_C^0 is the ice mass density at atmospheric pressure $p_C = 0$ and $T = T_f$.

According to our idealized pore model, ice can be created by: (i) heterogeneous nucleation from dispersed nucleating agents acting as catalyst sites; (ii) homogeneous nucleation in the range $T^* \simeq 233$ K; (iii) ice percolation through the channel connecting the pore to the material surface where heterogeneous nucleation is easier. The two first mechanisms relate to the left-hand side of Fig. 2, where r^* is the radius of the critical ice spherical nucleus; the last relates to the right-hand side, where r^* is the radius κ of the cylindrical channel through which the ice crystal percolates from the material surface. Whatever the actual process we assume that the pore crystallization eventually results from the coalescence of multiplying identical sites. As soon as the large pore is frozen, further ice formation within surrounding smaller pores requires the temperature to go down according to (1). This explains why ice formation in porous media is progressive owing to the pore size distribution. This also means that the case sketched out in the right-hand side of Fig. 2 can be located in the core sample, where pore freezing occurs from ice percolation through larger, already frozen, pores.

3. In-pore crystallization

According to linear isotropic elasticity the pore pressure p is related to the pore volume change according to

$$p = \frac{4}{3} G_S(\phi - 1) \tag{3}$$

where G_S is the matrix shear modulus and ϕ the ratio of the current volume and its undeformed one V. The crystal pressure p_∞ that would result from an instantaneous freezing of the whole pore liquid is:

$$p_\infty = \frac{4G_S K_C}{4G_S + 3K_C}\left(\frac{\rho_L^0}{\rho_C^0} - 1\right) \tag{4}$$

where K_J is the bulk modulus of phase $J = L, C$, which relates the current pressure p_J to the current mass density ρ_J, according to:

$$\frac{\rho_J^0}{\rho_J} = 1 - \frac{p_J}{K_J}; \quad \frac{\rho_J}{\rho_J^0} = 1 + \frac{p_J}{K_J}; \quad \frac{p_J}{K_J} \text{ and } \frac{\rho_L^0}{\rho_C^0} - 1 \ll 1 \tag{5}$$

For most materials (4) provides unlikely high values for the final pressure of the freezing pore, so that instantaneous freezing is questionable. Actually a progressive pore pressurization can expel a significant amount of liquid out of the pore, resulting in a final pressure much lower than p_∞. To the aim at assessing such a final pressure let $0 \leqslant \varphi(t) \leqslant 1$ be the mass fraction of the liquid water initially in the pore, which has transformed into ice at time t. According to our pore ice formation scheme the average pressure acting on the pore walls is:

$$p = \varphi(t)\, p_C + \big(1-\varphi(t)\big)\, p_L \tag{6}$$

The liquid mass υ, which flows out of the pore per unit of initial liquid mass of the pore, can then shown to be:

$$\upsilon = \left[\frac{\rho_L^0}{\rho_C^0} - 1 - \rho_C^0 \Delta\mu^* \left(\frac{1}{(4/3)G_s} + \frac{1}{K_C}\right)\right]\varphi(t) - \left(\frac{1}{(4/3)G_s} + \frac{\varphi(t)}{K_C} + \frac{1-\varphi(t)}{K_L}\right) p_L \tag{7}$$

To derive Eq. (7) we made use of (5), entailing $\rho_L^0 p_J / \rho_C^0 K_J \simeq p_J / K_J$ up to the second order. Assuming a Poiseuille flow in the connection channels, which separate the pore from the surrounding pores remaining at zero pressure, we write:

$$p_L = \eta \frac{\mathrm{d}\upsilon}{\mathrm{d}t}; \quad \eta = \frac{8LV}{n\pi a^4}\eta_L \tag{8}$$

where η_L is the water dynamic viscosity, n the number of channels, and L their length. (7) and (8) combine to give:

$$\big[1+\alpha\big(1-\varphi(t)\big)\big]\frac{\mathrm{d}\upsilon}{\mathrm{d}t} + \frac{\upsilon}{\tau} = \frac{1}{\eta}\big(p_\infty - \rho_C^0 \Delta\mu^*\big)\varphi(t), \quad \upsilon(0) = 0 \tag{9}$$

where $\alpha = (1/K_L - 1/K_C)/(3/4G_s + 1/K_C)$ and $\tau = \eta(3/4G_s + 1/K_C)$. Assuming a steady-state in-pore ice formation regime $\varphi(t) = \dot{\varphi} t$, the solution of (9) used conjointly with (2), (6) and (8) furnishes:

$$0 \leqslant t \leqslant 1/\dot{\varphi}: \quad p = \chi(t)\, p_\infty + \big(\dot{\varphi} t - \chi(t)\big)\rho_C^0 \Delta\mu^* \tag{10}$$

where $\chi(t) = (\dot{\varphi}\tau/(1-\alpha\dot{\varphi}\tau))(1 - ((1+\alpha-\alpha\dot{\varphi}t)/(1+\alpha))^{1/(\alpha\dot{\varphi}\tau)-1})$. Since we used (2), the pore freezing is assumed to occur sufficiently quickly with regard to the temperature decrease in order that the pressure difference $p_C - p_L$ and the temperature $T = T^*$ can be coinjointly set constant during the crystallization stage. The latter ends up at time $\theta = 1/\dot{\varphi}$, whose substitution in (10) provides the final pore pressure p_θ (see Fig. 3) and the underpressurization coefficient $0 \leqslant \chi_\theta \leqslant 1$

$$p_\theta = \chi_\theta\, p_\infty + (1-\chi_\theta)\rho_C^0 \Delta\mu^*; \quad \chi_\theta = \frac{\dot{\varphi}\tau}{1-\alpha\dot{\varphi}\tau}\big(1 - (1+\alpha)^{1-1/(\alpha\dot{\varphi}\tau)}\big) \tag{11}$$

For instantaneous freezing, $\dot{\varphi} \to \infty$, we recover $\chi_\theta = 1$ such that $p_\theta = p_\infty$. For infinitely slow pore freezing, $\dot{\varphi} \to 0$, so that $\chi_\theta = 0$ and $p_\theta = \rho_C^0 \Delta\mu^*$. For the whole range of freezing rates $p_\infty \geqslant p_\theta \geqslant \rho_C^0 \Delta\mu^*$. The actual

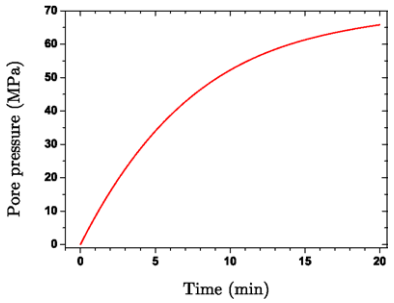

Fig. 3. Pore pressure evolution from freezing onset at 264 K. Complete pore freezing is achieved at $\theta = 20$ min such that $p_\theta \simeq \frac{1}{10} p_\infty \simeq 65.8$ MPa. Other values are $\alpha \simeq 2.81$ and $\tau \simeq 84$ s. This pressure value is quite high: however it does not impinge on the succeeding pore pressure relaxation and cryosuction (Fig. 4) that our analysis has revealed (Sections 4 and 5).

value of the underpressurization factor χ_θ can be determined from experimental data as the ones reported in Fig. 1, which provides the freezing temperature T^* and the freezing time $\theta = 1/\mathring{\varphi}$, while α and τ are material properties.

4. In-pore ice partial melting and pore relaxation

At times $t \geqslant \theta$ ulterior to pore complete freezing, the ongoing process can be analysed by letting $\varphi(t \geqslant \theta) = 1$ into (9) and by replacing the specific undercooling at crystallization $\rho_C^0 \Delta\mu^*$ by its current value $\rho_C^0 \Delta\mu = \mathcal{S}_f(T_f - T)$. A derivation of the resulting equation where we substitute (8), and use of the thermodynamic equilibrium equation (2) provide the equation governing the pressure of the frozen pore

$$t \geqslant \theta;\ T \leqslant T^*: \quad \tau \frac{\mathrm{d}p}{\mathrm{d}t} + p = \mathcal{S}_f(T_f - T); \quad p(t=\theta) = p_\theta \tag{12}$$

where pore pressure p now identifies to the ice crystal pressure. At a temperature remaining constantly equal to the freezing temperature T^*, (12) integrates in the form:

$$p(u = t - \theta \geqslant 0) = \rho_C^0 \Delta\mu^* + (p_\theta - \rho_C^0 \Delta\mu^*) \exp(-u/\tau) \tag{13}$$

According to the liquid water-crystal thermodynamic equilibrium equation (2) the second term on the right-hand side of (13) identifies to the liquid water pressure at the pore/channel entry. The liquid pressure prevailing at the end of the pore crystallization is $p_\theta - \rho_C^0 \Delta\mu^*$. It is positive for a non zero freezing rate. Actually it provokes a liquid flow from the frozen pore to the surrounding pores. As time goes by, the liquid water pressure progressively vanishes, owing to the Poiseuille flow supplied by the partial melting of the frozen pore. As a result the pore/crystal pressure goes progressively down to $\rho_C^0 \Delta\mu^*$, producing a pore relaxation.

5. Micro-cryosuction

Let now the temperature decrease below the pore freezing point, yet remaining larger that the temperature obtained by letting $r^* = a$ in (1) such that the channels remain unfrozen in the whole process depicted below. If the temperature drops linearly with time, $T(u \geqslant 0) = -\mathring{T}u + T^*$, (12) now integrates in the form:

$$p(u = t - \theta \geqslant 0) = \rho_C^0 \Delta\mu + \left[-\mathcal{S}_f \mathring{T}\tau + (\mathcal{S}_f \mathring{T}\tau + p_\theta - \rho_C^0 \Delta\mu^*) \exp(-u/\tau)\right] \tag{14}$$

where the current specific undercooling $\rho_C^0 \Delta\mu$ identifies to $p - p_L = \rho_C^0 \Delta\mu^* + \mathcal{S}_f \mathring{T}\tau$. The pore pressure relaxes up to time $t_m = \theta + \tau \ln((\mathcal{S}_f \mathring{T}\tau + p_\theta - \rho_C^0 \Delta\mu^*)/\mathcal{S}_f \mathring{T}\tau)$, where it is equal to $p_m = \rho_C^0 \Delta\mu_m$, before getting up again. This pressure rise can be explained as follows. According to the liquid water-crystal thermodynamic equilibrium (2), where T^* and p_C now stand for the current temperature T and pore pressure p, the term in brackets in (14) identifies to the decreasing current liquid water pressure at the pore/channel entry. As long as the latter is positive, the melting mechanism goes on in order to supply the liquid flow from the frozen pore to the surrounding pores. This stops at time t_m, where the liquid pressure is zero and the pore/crystal pressure becomes equal to the current specific undercooling. For times beyond t_m, the temperature drop carries on increasing, as well as the undercooling related to the surfused water in the channel. The liquid water-crystal thermodynamic equilibrium continues to be met provided that the difference between the liquid pressure at the pore/channel entry and the pore/crystal pressure goes on increasing. This is made possible only if simultaneously the liquid pressure becomes negative and the crystal pressure gets up. Actually the liquid pressure becoming negative, a micro-cryosuction process tends to restore a zero liquid pressure at the pore/channel entry, by drawing liquid water from the yet unfrozen surrounding porous network to the already frozen pore. This liquid water so pumped freezes when entering the pore, resulting in pore/crystal pressure increase. A steady state flow finally installs with p_L tending to $-\mathcal{S}_f \mathring{T}\tau$ as time goes to infinity.

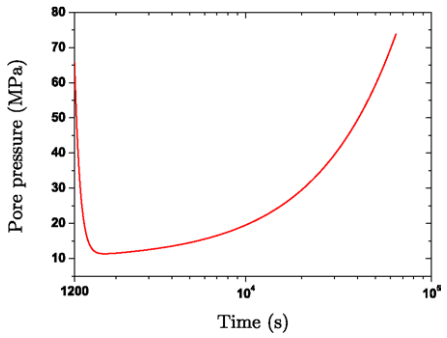

Fig. 4. Cement pore pressure evolution from complete pore freezing ($\theta = 1200$ s).

Such mechanism is facilitated by the existence of a very thin quasi-liquid layer (the physical and thermo-mechanical properties of this special water are however not very known [10]) between the crystal and the pore wall [4,11].

The pore relaxation and the succeeding microcryosuction are illustrated in Fig. 4 where we adopted the material and experimental values (which also served for Fig. 3): $\rho_L^0 = 0.9998$ g/cm^3, $\rho_C^0 = 0.9167$ g/cm^3 both at 273 K [10], $\eta_L = 1.793 \times 10^{-3}$ Pa s at 273 K [12], $K_L = 1.961 \times 10^9$ Pa at 273 K [13], $K_C = 8.65 \times 10^9$ Pa at 257 K [10], $\mathcal{S}_f = 1.2$ MPa/K at 273 K [10], $\gamma = 0.0409$ J/m^2 [2], $G_S = 30 \times 10^9$ Pa, $L = 250$ μm [14], $a = 1$ nm, $R = 500$ nm, $n = 1$, $1/\mathring{\varphi} = 20$ min at $T^* = 264$ K and $\mathring{T} = 3$ K/h [8]. Figs. 3 and 4 together finally account for the data reported in Fig. 1. The second expansion taking place from 241 K lasts approximatively 270 min and should involve homogeneous nucleation [6]. The subsequent observed contraction can be explained by the same in-pore ice partial melting mechanism.

Acknowledgement

The first author acknowledges the Miller Institute for Basic Research in Science, University of California Berkeley, as supporting this work, which he completed during the fall semester 2004 as a Visiting Miller Research Professor.

References

[1] J.J. Beaudoin, C. MacInnis, The mechanism of frost damage in hardened cement paste, Cement and Concrete Res. 4 (1974) 139–147.
[2] M. Brun, A. Lallemand, J.F. Quinson, C. Eyraud, A new method for the simultaneous determination of the size and the shape of pores: the thermoporometry, Thermochim. Acta 21 (1977) 59–88.
[3] G. Scherer, Freezing gels, J. Non-Crystalline Solids 155 (1993) 1–125.
[4] J.G. Dash, Haiying Fu, J.S. Wettlaufer, The premelting of ice and its environmental consequences, Rep. Progr. Phys. 58 (1995) 115–167.
[5] T. Powers, The air requirement of frost-resistant concrete, Highway Research Board, PCA Bulletin 33 29 (1949) 184–211.
[6] S. Béjaoui, E. Revertégat, J.P. Bournazel, Mécanismes de formation de la glace au sein des pâtes de ciment et des bétons, Rev. Française de Génie Civil 6 (2002) 1309–1332.
[7] B. Zuber, J. Marchand, Predicting the volume instability of hydrated cement systems upon freezing using poro-mechanics and local phase equilibria, Materials and Structures/Concrete Sci. Engrg. 37 (268) (2004) 257–270.
[8] V. Penttala, Freezing-induced strains and pressures in wet porous materials and especially in concrete mortars, Adv. Cement Bas. Mat. 7 (1998) 8–19.
[9] S. Taber, The mechanics of frost heaving, J. Geology 38 (1930) 303–317.
[10] V.F. Petrenko, R.W. Whitworth, Physics of Ice, first ed., Oxford University Press, 1999.
[11] G. Scherer, Crystallization in pores, Cement and Concrete Res. 29 (1999) 1347–1358.
[12] D.R. Lide (Ed.), Handbook of Chemistry and Physics 2001–2002, CRC Press, 2001.
[13] R.J. Speedy, Thermodynamic properties of supercooled water at 1 atm, J. Phys. Chem. 91 (1987) 3354–3358.
[14] J.-F. Ulm, G. Constantinides, F.H. Heukamp, Is concrete a poromechanics material? – A multiscale investigation of poroelastic properties, Material and Structures/Concrete Sci. Engrg. (December 2003).